JACS
JOURNAL OF THE AMERICAN CHEMICAL SOCIETY
Article
pubs.acs.org/JACS

Scope and Mechanism of Cooperativity at the Intersection of Organometallic and Supramolecular Catalysis

Mark D. Levin,[†] David M. Kaphan,[†] Cynthia M. Hong, Robert G. Bergman,* Kenneth N. Raymond,* and F. Dean Toste*

Chemical Sciences Division, Lawrence Berkeley National Laboratory and Department of Chemistry, University of California, Berkeley, California 94720, United States

Supporting Information

ABSTRACT: The scope and mechanism of the microenvironment-catalyzed $C(sp^3)-C(sp^3)$ reductive elimination from transition metal complexes [Au(III), Pt(IV)] is explored. Experiments detailing the effect of structural perturbation of neutral and anionic spectator ligands, reactive alkyl ligands, solvent, and catalyst structure are disclosed. Indirect evidence for a coordinatively unsaturated encapsulated cationic intermediate is garnered via observation of several inactive donor-arrested inclusion complexes, including a crystallographically characterized encapsulated Au(III) cation. Finally, based on stoichiometric experiments under catalytically relevant conditions, a detailed mechanism is outlined for the dual supramolecular and platinum-catalyzed C−C coupling between methyl iodide and tetramethyltin. Determination of major platinum species present under catalytic conditions and subsequent investigation of their chemistry reveals an unexpected interplay between cis−trans isomerism and the supramolecular catalyst in a Pt(II)/Pt(IV) cycle, as well as several off-cycle reactions.

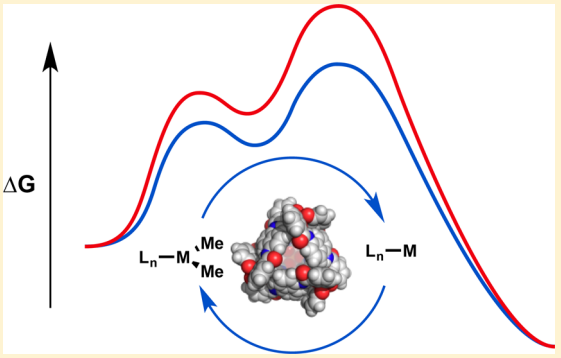

INTRODUCTION

Recognition of the role played by ligand architecture in determining the reactivity of transition metal catalysts revolutionized organotransition metal chemistry and allowed the proliferation of previously inaccessible catalytic processes, yielding methodologies with remarkable activity, selectivity, and efficiency.[1,2] Central to this advance is the ability to modulate the catalyst's local microenvironment, both steric and electronic, as a means to influence the rates of individual elementary steps, control catalyst speciation, and disfavor deactivation pathways. However, in employing this approach, one necessarily defines the same microenvironment to the transition metal center throughout the course of the catalytic cycle, often resulting in a trade-off between elementary steps, wherein a ligand architecture may accelerate a step of interest at the expense of another on-cycle reaction.

This limitation is circumvented if a microenvironment is applied uniquely to a single elementary step via the selective recognition of a particular catalytic intermediate and its subsequent transition state by transient encapsulation within a supramolecular cocatalyst (Figure 1).[3,4] In such an approach, the microenvironment of the transition metal catalyst can be defined differentially for one step of the catalytic cycle. Our group recently reported a realization of this strategy, employing a union of supramolecular and transition metal catalysis to selectively accelerate the rate-determining step within a cross-coupling catalytic cycle.[5]

In the initial report, supramolecular microenvironment catalyst **1** (Figure 1) was shown to dramatically accelerate the C−C reductive elimination from high-valent [Au(III), Pt(IV)] metal alkyl complexes. This capacity was rendered into a dual-catalytic $C(sp^3)-C(sp^3)$ coupling in which the cooperative action of both a platinum and supramolecular catalyst was required for efficient turnover.[5] The substantial effect of the supramolecular catalyst prompted us to examine the structure−reactivity relationships involved in greater detail, as a means to better ascertain the nature of the interaction between these two catalytic manifolds.

The self-assembled $K_{12}(Ga_4L_6^{12-})$ [L = *N,N′-bis*(2,3-dihydroxybenzoyl)-1,5-diaminonaphthalene] supramolecular assembly **1** is a tetrahedral cluster comprised of four pseudooctahedral gallium *tris*(catecholate) vertices bridged by *bis*-bidentate ligands.[6] Due to mechanical coupling, **1** assembles as a racemic mixture of diastereomerically pure ΔΔΔΔ and ΛΛΛΛ isomers. Related cluster **2** is decorated at the vertices with chiral amide functionality, which imparts increased thermal and oxidative stability to the cluster.[7] Rapid and reversible guest encapsulation occurs via an aperture dilation mechanism, and both neutral and cationic guests have been observed to bind with high affinity.[8]

Guest molecules within **1** experience a diagnostic upfield shift in ^1H NMR resonances of up to 3 ppm due to close

Received: May 26, 2016
Published: July 26, 2016

DOI: 10.1021/jacs.6b05442
J. Am. Chem. Soc. 2016, 138, 9682−9693

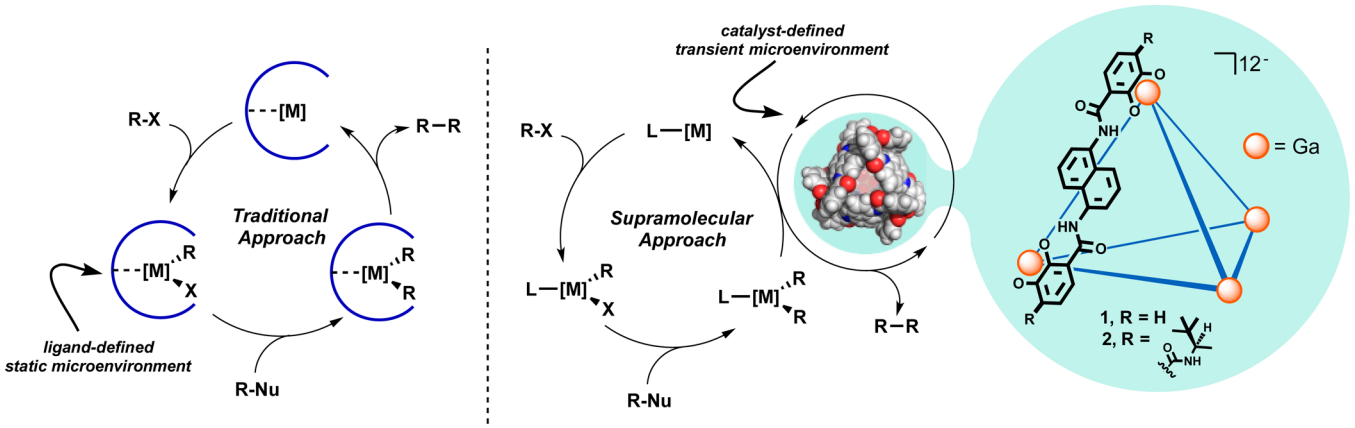

Figure 1. A supramolecular approach for transition metal catalyzed cross-coupling.

contact with the ring current of the flanking naphthalene walls, which allows for convenient identification of encapsulated species.[6] The enzyme-like binding pocket also modulates the properties of guests encapsulated within cluster **1**, with an observed pK_a shift for amines and phosphines, decreasing their basicity by up to 4 orders of magnitude.[9] Furthermore, **1** is capable of noncovalent recognition of several cationic transition states, having been shown to catalyze a variety of Brønsted acid mediated and cyclizative transformations.[10] Cluster **1** also effectively encapsulates transition metal complexes via concomitant heterolysis of a metal–halogen bond.[11]

INITIAL FINDINGS

Capitalizing on the recognition of cationic transition states and binding of transition metal complexes, we previously disclosed the catalysis of alkyl–alkyl reductive elimination from Au(III) complex **3-I** (eq 1) and Pt(IV) complex **5** (eq 2).[5,12,13] The

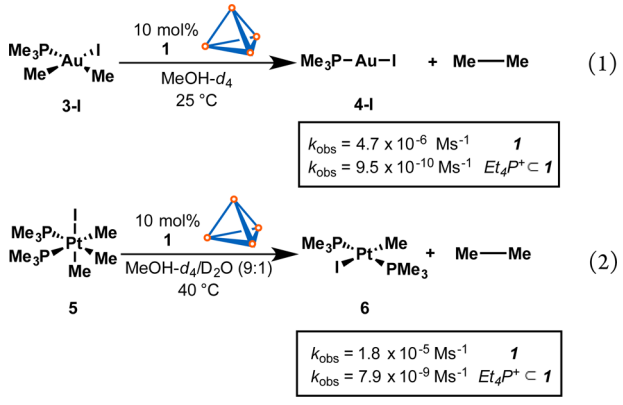

(1)

(2)

rates in the presence of 10 mol % **1** were substantially faster than those of the corresponding background reactions (measured by blocking the binding pocket of **1** with the strongly bound guest Et_4P $B(Ar_F)_4$ [Ar_F = 3,5-bis(trifluoromethyl)phenyl]), with 4000- and 2300-fold differences in the observed rate, respectively.[14]

Kinetic experiments on both Au and Pt complexes by the method of initial rates showed first-order dependence on **1**, inhibition by exogenous iodide, and saturation in the transition metal substrate. These results were consistent with a Michaelis–Menten-like mechanism, involving preequilibrium dissociation of halide and encapsulation by the supramolecular host complex followed by rate-limiting reductive elimination (Scheme 1).

Scheme 1. Mechanism of Cluster Catalyzed Reductive Elimination[5]

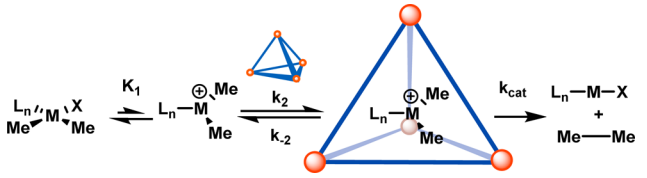

Lineweaver–Burk analysis afforded the rate of reductive elimination within the supramolecular assembly (k_{cat}), with measured values of 3.3 × 10^{-2} s^{-1} for **3** and 2.4 × 10^{-2} s^{-1} for **5** corresponding to accelerations (k_{cat}/k_{uncat}) of 5.0 × 10^5 and 2.6 × 10^4 respectively.[15]

INFLUENCE OF SPECTATOR LIGANDS

In our initial report, we also noted the dramatic influence of the neutral phosphine ligand on the cluster-catalyzed reductive elimination of ethane from Au(III).[5] The triethylphosphine ligated complex **7-I** undergoes catalyzed reductive elimination with a half-life 68 times shorter than that observed for the trimethylphosphine analogue (47 s vs 53 min) as shown in eq 3.[16] This is in stark contrast to the approximately 4-fold difference in the *uncatalyzed* rates that is observed.

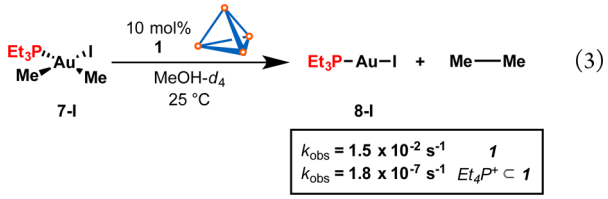

(3)

Indeed, as determined by Michaelis–Menten analysis, the measured rate of reductive elimination within the supramolecular assembly (k_{cat}) is 38 times faster for **7** than for **3** and is the highest acceleration over background observed to date for any synthetic supramolecular catalyst (k_{cat}/k_{uncat} = 1.9 × 10^7).

A more detailed analysis of the relative rate constants for reductive elimination from **3-I** and **7-I** reveals that **7-I** is bound more tightly by **1** and, after the binding event, the transition state for reductive elimination from **7-I** is effectively more

DOI: 10.1021/jacs.6b05442
J. Am. Chem. Soc. 2016, 138, 9682–9693

stabilized by **1** than is the transition state of reductive elimination from **3-I**. Comparison of the ratio of catalyzed observed rates (68-fold corresponding to $\Delta\Delta G^{\ddagger}$ = 2.5 kcal/mol) to the ratio of k_{cat} (38-fold corresponding to $\Delta\Delta G^{\ddagger}$ = 2.2 kcal/mol) suggests that the triethylphosphine ligated complex shows higher binding affinity for the interior of **1** ($\Delta\Delta G$ = 0.3 kcal/mol). Furthermore, comparison of the ratio of background rates of reductive elimination from **3-I** and **7-I** (3.8-fold corresponding to $\Delta\Delta G^{\ddagger}$ = 0.79 kcal/mol) to the ratio of the catalyzed rate of reductive elimination suggests that **1** more effectively stabilizes the transition state for reductive elimination from the triethylphosphine ligated complex ($\Delta\Delta\Delta G^{\ddagger}$ = 1.7 kcal/mmol). For a graphical depiction of this analysis, see the Supporting Information (Figure S7).[17]

Several possible explanations for this phenomenon are consistent with the experimental results: (i) increased steric compression of the larger complex within the supramolecular cavity (thus destabilizing the bound ground state relative to the transition state for reductive elimination),[1] (ii) increased hydrophobicity due to Et_3P,[8b] (iii) better shape complementarity resulting in better solvent exclusion and increased contact surface area,[18] or (iv) higher concentrations of the free cationic Au(III) complex as a result of the stronger electron donation from the triethylphosphine ligand.[2a]

A second salient difference between **3-I** and **7-I** is their behavior at extended reaction times (Figure 2). Consumption of **3-I** deviated from first-order decay, concurrent with a buildup of two signals in the upfield region of the ^{1}H NMR spectrum (indicative of a strongly encapsulated complex). In contrast to this, **7-I** showed clean first-order behavior, with no catalyst deactivation observed.

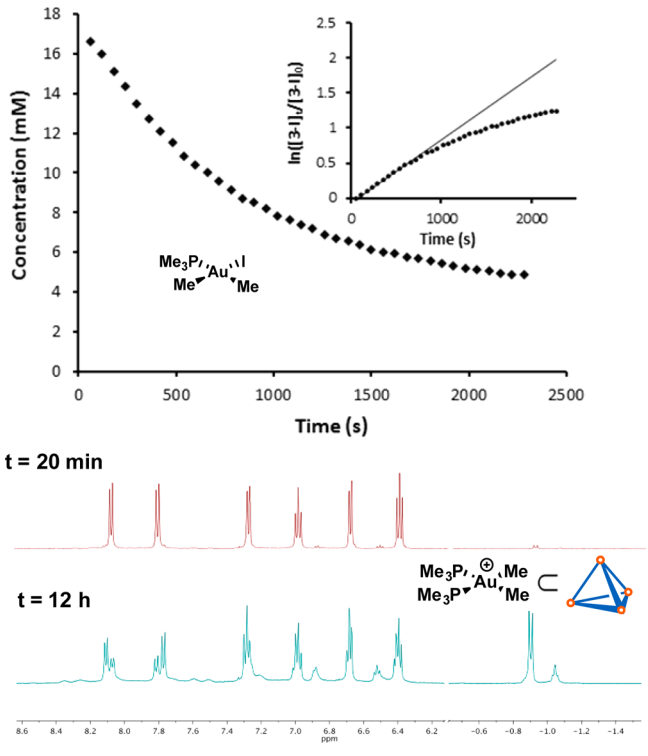

Figure 2. Reaction profile for reductive elimination of **3-I** catalyzed by **1** at 35 °C with inlaid natural log plot showing deviation from first-order decay (top), and ^{1}H NMR spectrum at extended reaction times showing a deactivated catalyst with a strongly encapsulated guest (bottom).

The guest complex formed in the reaction of **3-I** was consistent with bis(trimethylphosphine) gold cation **9** ⊂ **1**, which was verified by encapsulation of independently synthesized **9** (eq 4).[19]

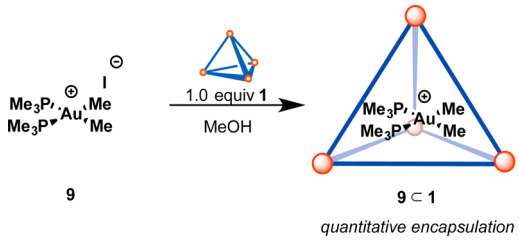

(4)

In contrast, the rate of reductive elimination from triphenylphosphine congener **10** is uninfluenced by the presence of a catalytic amount of **1**, indicative of size exclusion from the binding pocket of the supramolecular catalyst (eq 5). This phenomenon has been well-documented in the context of both supramolecular and enzymatic catalysis.[20,21]

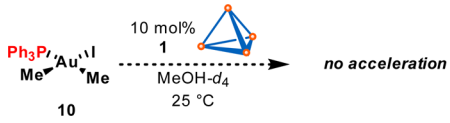

(5)

The identity of the halide substituent on **3** also has a dramatic effect on the rate of the reaction, as well as the catalyst deactivation pathways. Examination of the iodide, bromide, and chloride congeners **3-I**, **3-Br**, and **3-Cl** revealed a significant influence on the observed rate of 1-catalyzed reductive elimination, with the relative rates increasing in the order Cl ≈ Br > I (Figure 3). We also observed product inhibition from encapsulation of the resulting Au(I) complexes **4-Cl** and **4-Br** but not for **4-I**.

In order to determine the generality of this behavior, the corresponding triethylphosphine ligated analogues **7-Cl** and **7-Br** were prepared and subjected to cluster catalyzed reductive elimination. The results showed significant product inhibition by **8-Cl** and **8-Br**, with substantial deviation from first-order decay. In contrast, **7-I** and its product **8-I** followed an uninhibited first-order reaction profile past five half-lives (Figure 4). Indeed, the rapid rate of the reaction and sheer extent of product inhibition in the case of **7-Cl** and **7-Br** precluded a quantitative comparison of the initial rate differences between this halide series. However, the qualitative trend for overall reaction rate of Cl ≈ Br > I is consistent between the **3-X** and **7-X** series.

Based on the proposed mechanism for cluster catalyzed reductive elimination, one would expect pre-equilibrium halide dissociation to influence the overall rate. However, *a priori*, the direction of this influence is unclear. Examination of a generalized equilibrium for encapsulation reveals that the empty cluster and encapsulated cation are identical for all members of the series, and as such only the Au−X heterolytic bond dissociation energies and differences in solvation of the dissociated halide anion can influence the position of the equilibrium. For Au(III) the Au−X heterolytic bond strengths trend as Au−I < Au−Br < Au−Cl,[22] while solvation enthalpy of the dissociated halides[23] trends as Cl > Br > I. Clearly the observed rates for reductive elimination for **3** (Cl ≈ Br > I)

DOI: 10.1021/jacs.6b05442
J. Am. Chem. Soc. 2016, 138, 9682−9693

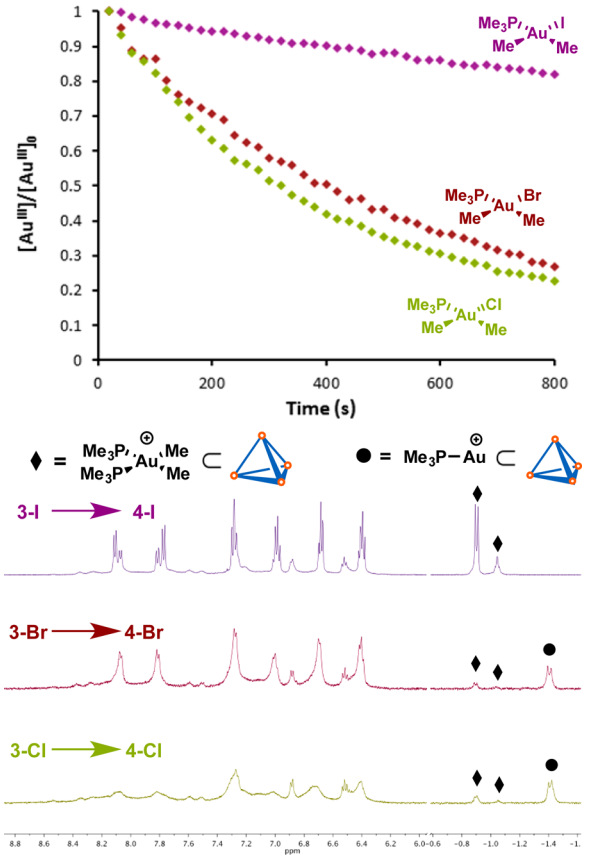

Figure 3. Reaction traces for reductive elimination from **3-I**, **3-Br**, and **3-Cl** catalyzed by **1** (top), and ^{1}H NMR spectrum showing product inhibition at long reaction times by **4-Br** and **4-Cl** (bottom).

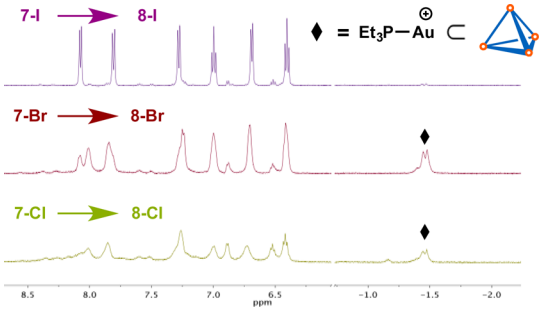

Figure 4. ^{1}H NMR spectrum showing product inhibition by **8-Br** and **8-Cl**, with no encapsulation observed for **8-I**.

correlate more strongly with the halide solvation enthalpy than the relevant Au(III) halide bond strengths (one would expect the gold chloride complexes to undergo slower reductive elimination in that case).

For Au(I), the relative influence of solvation and bond strength is less clear. The heterolytic bond strengths trend as Au–Br < Au–Cl < Au–I.[23] Here, the observation of product inhibition in the case of the bromide and chloride Au(I) complexes is consistent with both solvation-dependent and bond-strength-dependent equilibria for encapsulation of **4-X** and **8-X**, but the observation of solvation-dominated behavior for Au(III) suggests that the influence of solvation is likely also the major factor in this trend. Additionally consistent with this explanation is the observation that increasing the water content of the solvent resulted in a corresponding increase in reaction rate (see SI for details).

NATURE OF THE MICHAELIS COMPLEX

While kinetic investigations of the catalytic reductive elimination process reveal a Michaelis–Menten-like mechanism reminiscent of enzymatic catalysis, these data reveal little about the nature of the organometallic species undergoing reductive elimination; in the case of reductive elimination from platinum complex **5**, C–C bond formation might occur from a pentacoordinate intermediate, or alternatively from the hexacoordinate solvento complex.

Reductive elimination has previously been observed from hexacoordinate d^6 and square planar d^8 metals both with and without prior ancillary ligand dissociation in different cases, suggesting that either pathway might be competent.[1,12,25,26] While direct observation of this transient intermediate is precluded, some insight into its nature may be gained from the introduction of appropriate nonsolvent neutral donors.

Indeed, serendipitous donor-arrested reductive elimination was first observed as a cluster deactivation pathway in the catalyzed reductive elimination from **3-I** (*vide supra*). In contrast to the transient substrate–host complexes which rapidly undergo reductive elimination, the deactivated inclusion complex **9** ⊂ **1** was persistent enough to allow characterization by single-crystal X-ray diffractometry. Suitable crystals of complex **9** ⊂ **1** were obtained by vapor diffusion of acetone into a solution of the complex in 1:1 water and methanol over 2 weeks (Figure 5). Due to limited crystal size and a high degree

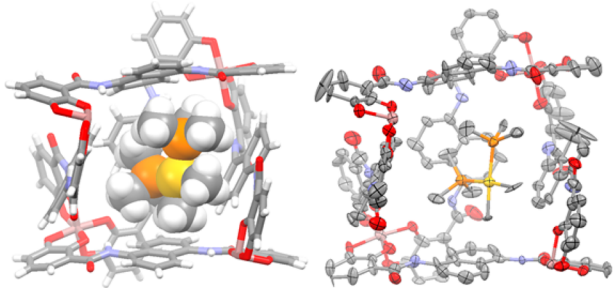

Figure 5. Crystal structure of **9** ⊂ **1**, space-filling model (left), and thermal ellipsoids (50% probability, right). Potassium ions, solvent, and one ligand of **1** have been removed for clarity.

of solvent disorder, synchrotron radiation was required to collect a sufficient data set at 0.88 Å resolution with 1.2276 Å radiation. Complex **9** ⊂ **1** crystallized in the monoclinic space group $P2_1/c$ with 4 formula units per unit cell, and the data are consistent with a molecule of **9** encapsulated within the cavity of **1**.[11e,18] Further crystallographic information can be found in the Supporting Information.

Similarly, the addition of exogenous neutral ligands to a solution of **5** and cluster **1** inhibited the catalyzed reductive elimination and afforded the corresponding high valent cationic inclusion complexes. A small excess of either trimethylphosphine or dimethylsulfide both effected the uptake of the cationic Pt(IV) after displacement of the iodide ligand to form a kinetically stable 1:1 host–guest complex (Figure 6).[27] These inclusion complexes were persistent even upon heating over 48 h, with no detectable reductive elimination observed. In the absence of cluster **1**, no iodide displacement could be detected by ^{1}H NMR in the presence of dimethylsulfide, and only slow,

DOI: 10.1021/jacs.6b05442
J. Am. Chem. Soc. 2016, 138, 9682–9693

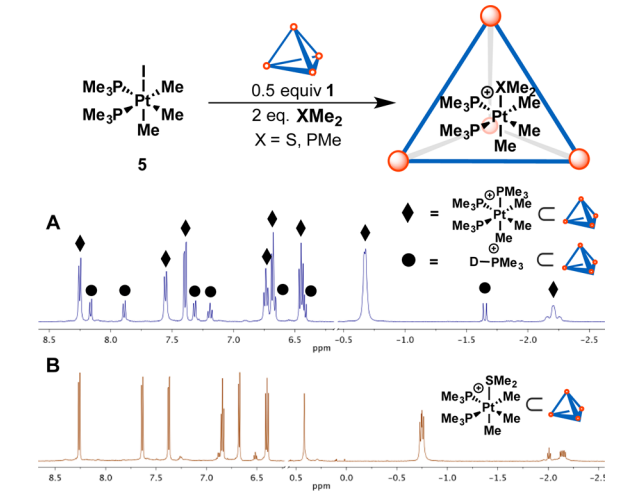

Figure 6. Donor-arrested complexes derived from trimethylphosphine and dimethylsulfide. (A) MeOD/D_2O 8:2, (B) pure MeOD.

partial displacement was observed with trimethylphosphine alone. In contrast, added trimethylamine had no effect on **5** or the supramolecular cluster, and the catalyzed reductive elimination proceeded unabated, a phenomenon that likely reflects the low innate affinity of platinum for amine donors.

Surprisingly, carbon monoxide was capable of displacing iodide from **5** to form a hexacoordinate inclusion complex within **2** (albeit with only partial occupancy of **2**, indicating a lower overall association constant). This observation was made quite unexpectedly in the context of an attempted carbonylative coupling (*vide infra*), where no reactivity was observed, due to the encapsulation of the cationic Pt(IV) carbonyl **11** (Figure 7).[27] While Pt(IV) carbonyl complexes have been previously

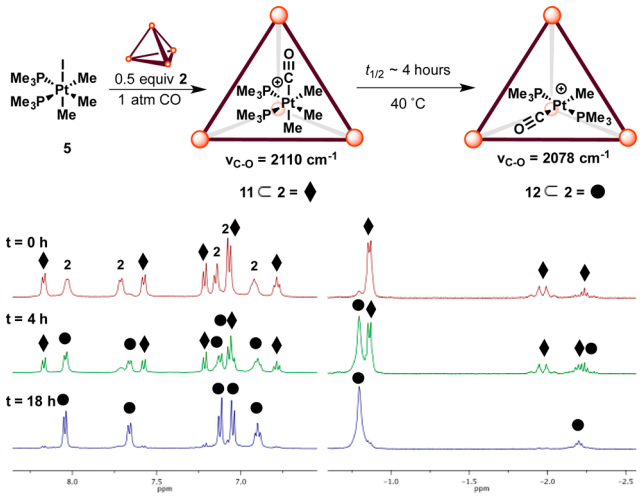

Figure 7. Carbon monoxide trapping of the Michaelis complex and slow reductive elimination.

observed, their rarity can be attributed to the paucity of electron density available for backdonation to carbonyl antibonding orbitals, underscoring the ability of **2** to perturb otherwise unfavorable equilibria.[28] Indeed, the IR spectrum of **11** ⊂ **2** showed a C═O stretch at ν = 2110 cm^{-1}, indicative of a relatively strong CO bond. Heating **11** ⊂ **2** at 40 °C effected reductive elimination of ethane with a half-life of about 4 h to afford the corresponding cationic Pt(II) carbonyl **12** (ν_{CO} = 2078 cm^{-1}). Clearly, a variety of neutral donors are capable of trapping the high valent cationic platinum intermediate to form a persistent inclusion complex within the cavity of the supramolecular cluster.

The fact that these hexacoordinate cationic species, even with donors as weak as carbon monoxide, undergo substantially inhibited reductive elimination compared to the parent catalytic process provides evidence by analogy that the putative oxygen coordinated solvento complex is unlikely to be the relevant species undergoing carbon−carbon bond formation. We therefore favor a model in which the coordinatively unsaturated pentacoordinate cationic metal complex undergoes reductive elimination within the cavity of the supramolecular assembly.

SCOPE OF THE REDUCTIVE ELIMINATION

Despite the noted influence of the spectator ligands, the actively transformed ligands are of greatest interest in the overall process. In order to glean further mechanistic insights as well as to determine the scope of cluster catalyzed reductive elimination, a sampling of typical functionality was examined.

Diethyl gold complex **13**, in the presence of 10 mol % of cluster **1**, underwent catalyzed reductive elimination to form butane with an observed rate constant of 7.6 × 10^{-3} s^{-1}, a relative rate of 29 when compared to catalyzed reductive elimination from dimethyl gold complex **3-I** (k_{obs} = 2.6 × 10^{-4} s^{-1}) (eq 6).

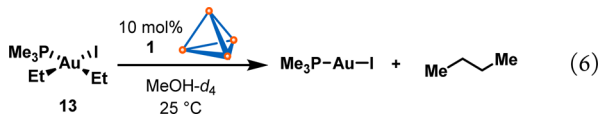

The consumption of ethyldimethyl platinium complex **14** was also accelerated dramatically in the presence of cluster **1**; however, instead of observing carbon−carbon bond formation, the exclusive organic products of the reaction were methane and ethylene (eq 7).[29] These products arise from β-hydride

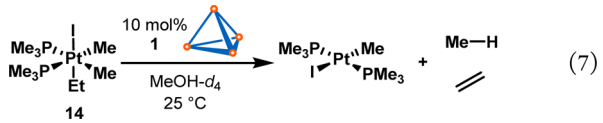

elimination from the pentacoordinate cationic encapsulated species to release ethylene, and subsequent methyl-hydrogen reductive elimination to form methane.[30] The catalyzed process took place with a half-life around 1 h, while, in the uncatalyzed reaction, only trace β-hydride elimination was observed after 16 h.

The acceleration of β-hydride elimination from **14** indicates that the intrinsic reactivity preferences of the metal are not overridden by the cluster; however, it highlights the fact that other elementary transformations are also subject to catalytic acceleration by **1**, so long as they also proceed through cationic transition states.

Acyl dimethyl platinum complex **15** undergoes reductive elimination, catalyzed by cluster **1**, to form acetone. The observed 15-fold acceleration over background in this case is modest relative to the aforementioned C(sp^3)−C(sp^3) reductive eliminations, with an initial rate of 2.2 × 10^{-3} s^{-1} in the presence of 10 mol % cluster and 1.5 × 10^{-4} s^{-1} in the background reaction (eq 8).[30] This can be explained by the relatively low barrier to reductive elimination in the uncatalyzed

DOI: 10.1021/jacs.6b05442
J. Am. Chem. Soc. 2016, 138, 9682−9693

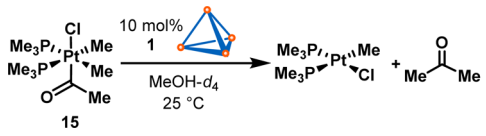

(8)

reaction for the sp^2-hybridized and electron-deficient acyl group. In this case, the kinetic product is the *cis*-chloroplatinum complex, but it undergoes isomerization to the *trans* isomer after reductive elimination.

On the other hand, reductive elimination from benzyl substituted platinum complex **16** was not accelerated in the presence of cluster **1** (eq 9).[29] The lack of catalytic activity in

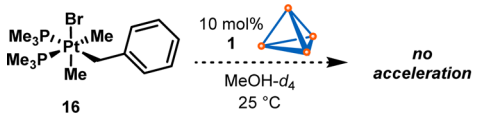

(9)

this case is most likely explained by a size exclusion phenomenon (similar to **10**, *vide supra*), where the benzyl group renders the complex too bulky to be encapsulated by the cluster.

Electronically similar allyl platinum complex **17**[29] also did not undergo catalyzed reductive elimination; however, a platinum species, consistent with the η^3-allyl platinum(IV) complex **18**, was observed as a strongly bound guest in the cluster cavity. The chiral cis-dimethyl η^3-allyl platinum cation is kinetically trapped as a diastereomeric mixture within the homochiral T-symmetry cluster. However, after 24 h, the complex isomerizes to favor the achiral trans-dimethyl η^3-allyl platinum cation **19** as the thermodynamic product (Figure 8).[27,31] The equilibrium mixture of **18** ⊂ **1** and **19** ⊂ **1** was

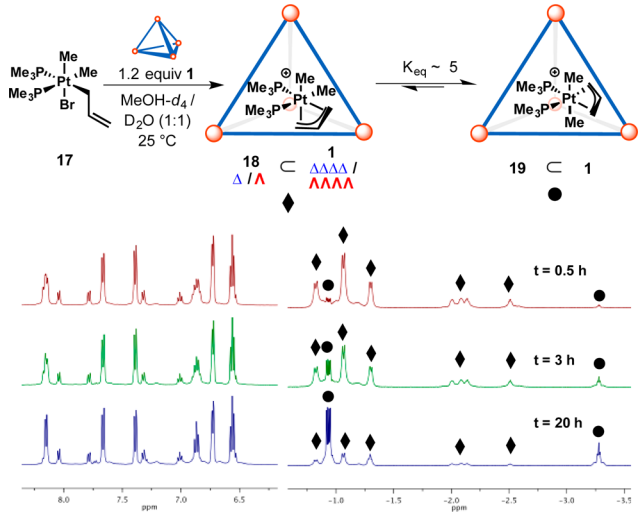

Figure 8. η^3 allyl complexes formed upon encapsulation of **17**.

persistent, with no reductive elimination observed even after heating to 45 °C for 48 h. For encapsulated **18**, reductive elimination is decelerated relative to the background reaction, which may be viewed as a case of intramolecular donor arrested reductive elimination, analogous to the previously observed behavior in the presence of exogenous neutral donors. For a similar allyldimethyl complex, Puddephatt and co-workers were unable to observe an η^3-allyl complex by treatment with $AgPF_6$. Instead, disproportionation products following reductive elimination were observed highlighting the divergent behavior enabled by the microenvironment of **1**.[30]

To probe the limits of the intramolecular donor-arrested reductive elimination, the homologated series of butenyl, pentenyl, and hexenyl platinum(IV) complexes **20**, **21**, and **22** were investigated (Figure 9). Unfortunately, the high

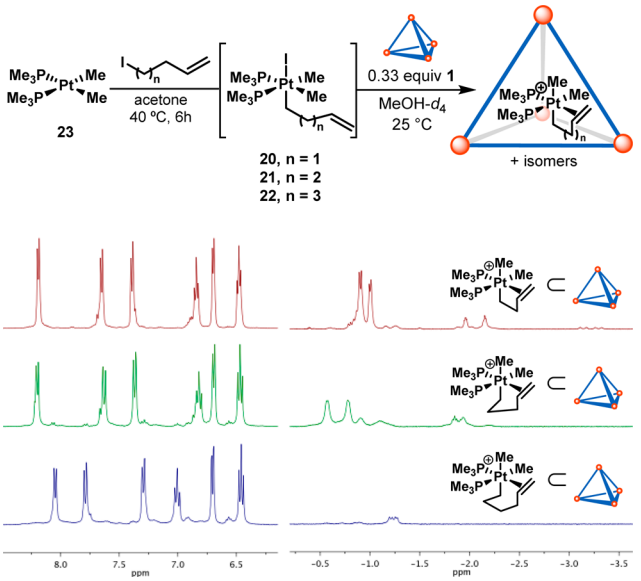

Figure 9. Homologous series of cyclic alkene-coordinated encapsulated platinum complexes.

propensity of these complexes to undergo β-hydride elimination prevented their isolation and purification. To circumvent this, the platinum(IV) complexes were generated in situ, followed by treatment with cluster **1**. The butenyl and pentenyl complexes were strongly encapsulated, and while both inclusion complexes were persistent on the time scale of days, the broadened ^{1}H NMR resonances in the encapsulation region for pentenyl complex **21** ⊂ **1** suggest that it is less strongly bound than the butenyl analogue. Conversely, only trace encapsulation of hexenyl analogue **22** is observed after 30 min at ambient temperature, and no species are encapsulated after 12 h with background formation of products from β-hydride elimination observed. This trend can potentially be explained as the result of several phenomena, including (i) conformational strain of the expanded ring complexes, (ii) the entropic cost of folding the homologated chains to bring the donor olefin into contact with the Pt cation, and (iii) size exclusion of the less compact complexes.

DUAL CATALYSIS

With the influence of various factors in the supramolecular catalysis of reductive elimination elucidated, we turned our attention to the dual supramolecular and platinum catalyzed cross-coupling reaction which evolved from this stoichiometric precedent. As reported previously, catalyst **2** in combination with precatalyst **23** enables the cross-coupling of methyl iodide and tetramethyltin to provide ethane (Figure 10).[5] The reaction requires the addition of fluoride, due to the strong encapsulation of the trimethyltin iodide byproduct. Under these conditions, the supramolecular catalyst exerts a dramatic effect on the reactivity of the platinum catalyst, with substantially slower conversion in its absence.

DOI: 10.1021/jacs.6b05442
J. Am. Chem. Soc. 2016, 138, 9682−9693

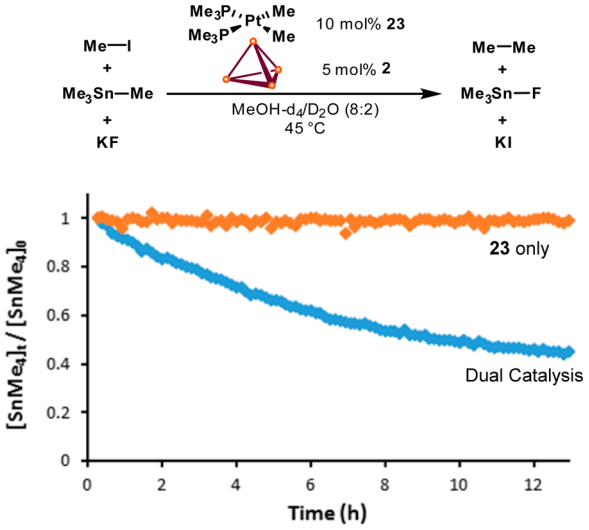

Figure 10. Dual supramolecular and transition metal catalysis in the C−C coupling of tetramethyltin and methyl iodide.[5]

INFLUENCE OF THE SUPRAMOLECULAR CATALYST

For the dual catalytic reaction, it was necessary to employ a modified supramolecular catalyst **2**, bearing electron-withdrawing amide substituents on the catecholate ligands bound to gallium. This was implemented as a means to increase the stability of the supramolecular catalyst to the methyl iodide substrate, but could potentially have an influence on the rate of catalyzed reductive elimination.

In order to explore this possibility, the rate of reductive elimination of both Au complex **3-I** and Pt complex **5** catalyzed by **2** was measured. In each case, **2** was found to give an observed rate of reductive elimination approximately 1.5 times faster than that of **1**. Similar relative rates have previously been measured for transformations catalyzed by **1** and **2**.[32]

Interestingly, the reductive elimination of **3-I** catalyzed by **2** does not deviate from first-order behavior, with no bis(phosphine) inclusion complex (**9** ⊂ **2**) detected (Figure 11).

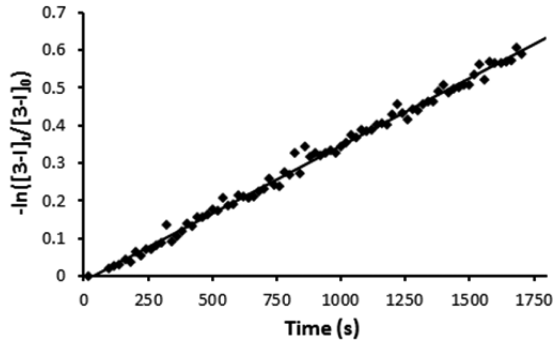

Figure 11. Clean exponential behavior for the reductive elimination from **3-I** catalyzed by **2**.

One possible explanation is that **9** is formed from trimethylphosphine liberated upon oxidation of the supramolecular catalyst by **3-I** or **4-I**, and the decreased electron density of the catecholate ligands on **2** relative to **1** slows this deleterious side reaction.

Catalyst **2** was also found to serve as a more robust catalyst in the reductive elimination from **7-I**, with a turnover number (TON) of 947, compared to the measured TON of 312 for complex **1**. Though the catalyst deactivation pathway in this case is unknown, it again seems plausible that **1** and **2** are oxidized by **8-I** and that the less electron-rich catecholate ligands are less susceptible to oxidation. This is supported by the formation of Au^0 precipitate after a large number of turnovers with **1** but not with **2**.

MECHANISM OF DUAL CATALYSIS

The observation of a dual supramolecular and platinum catalyzed cross-coupling between an alkyl stannane and an alkyl halide led us to interrogate the mechanism by which this process occurs. Namely, despite the presumed involvement of our stoichiometrically validated supramolecular catalysis of the C−C reductive elimination, the remaining elements of the catalytic cycle remained unclear. For one, limited precedent for transmetalation of alkyl stannanes to phosphine-supported platinum existed, and any additional role of fluoride (originally added to scavenge trimethytin iodide[5]) in this step was unclear.[33] Beyond this, oxidative addition of methyl iodide has been reported to both mono- and dialkyl Pt(II) complexes, suggesting that either pathway might be relevant.[30]

We began our investigation by identification of the major platinum species present under the dual-catalytic conditions starting from the precatalyst **23**. By a combination of ^{1}H and ^{31}P NMR, we identified four species, which were definitively assigned by independent synthesis as the Pt(II) complex **6**, and the three Pt(IV) complexes **5**, **24**, and **25** (Figure 12). While **5**

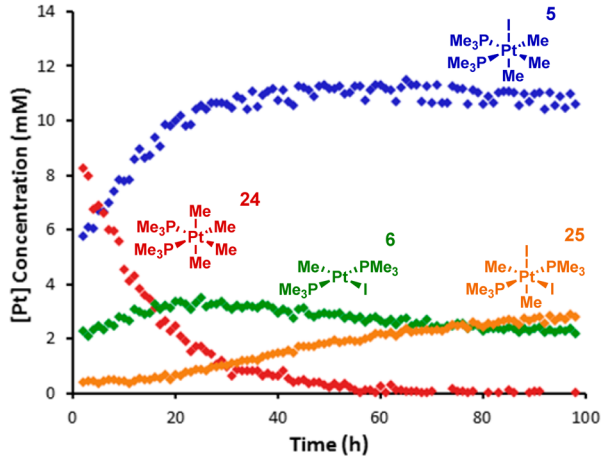

Figure 12. Concentration of major platinum species under dual catalytic conditions determined by ^{1}H NMR.

and **6** were not unexpected considering their role in the above stoichiometric reactivity, the involvement of **24** and **25** was less easily accommodated by our initial mechanistic hypothesis. The concentrations of these species over the course of the reaction is shown in Figure 12. While **6** maintains a roughly steady concentration, the initial burst and subsequent decay of **24** is accompanied by the growth in concentration of **5**, with **25** growing in gradually at late reaction times.[34]

In order to understand the origin of these species, we undertook a series of stoichiometric experiments, beginning with an investigation into the formation of tetramethylplatinum(IV) complex **24**.[24,35] Treatment of **5** with tetramethyltin under catalytically relevant conditions led to no reaction (eq 10). However, addition of potassium fluoride to the same

DOI: 10.1021/jacs.6b05442
J. Am. Chem. Soc. 2016, 138, 9682−9693

mixture resulted in rapid transmetalation to generate **24** and trimethyltin fluoride (eq 11). Surprisingly, this process was found to be reversible, and in the presence of trimethyl tin fluoride and potassium iodide, **24** was found to undergo conversion to tetramethyltin and **5** (eq 12).[36,37]

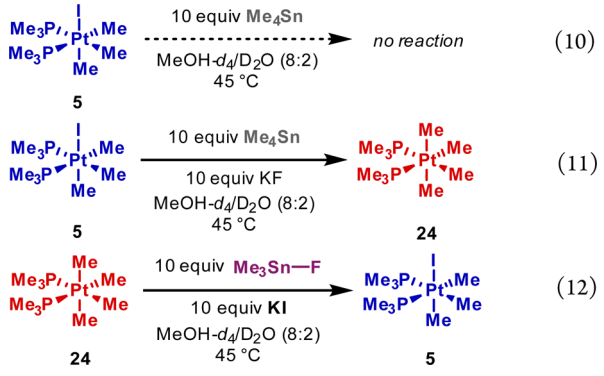

These results suggest a dynamic Pt(IV)/Sn transmetalation equilibrium mediated by fluoride, in which the relative concentrations of the four species dictate the overall distribution. This dynamic equilibrium can be readily observed by ^{1}H NMR under our catalytic conditions by comparing the relative concentrations of trimethyltin fluoride/tetramethyltin and **5**/**24** (Figure 13); at early reaction times, **24** is a major

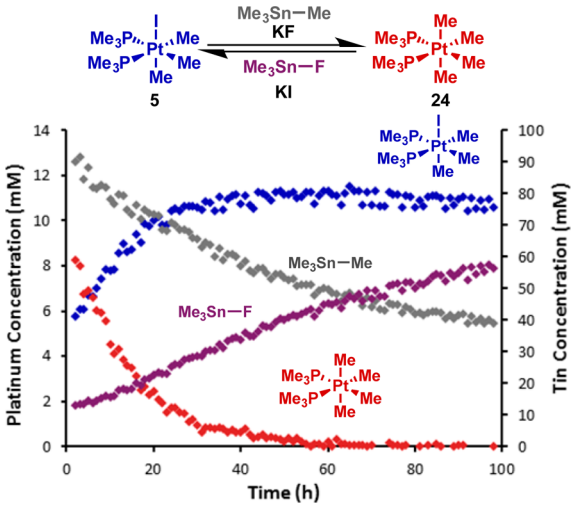

Figure 13. Dynamic transmetalation equilibrium between **5** and **24** under dual catalytic conditions.

species due to the high concentration of tetramethyltin, but as the reaction proceeds, tetramethyltin is consumed and trimethyltin fluoride is produced, pushing the equilibrium back toward **5**.

Having established the likely origin of **24**, we turned our attention to the fate of the Pt(II) complex **6**. Similar transmetalation experiments indicated that tetramethyltin was unreactive with **6** in either the presence or absence of potassium fluoride on catalytically relevant time scales (eq 13). However, it was observed that an equimolar mixture of **6** and **24** resulted in formation of **5** and **23** (eq 14). The kinetic product of transmetalation is the *trans*-dimethylplatinum(II) complex **28** (*vide infra*), but it undergoes isomerization to the *cis* isomer. The overall process was found to be reversible, suggesting a possible Pt(IV)/Pt(II) transmetalation equilibrium.

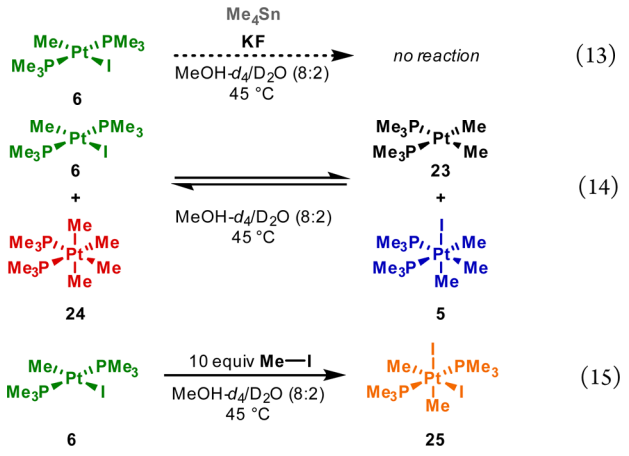

However, **6** was additionally found to undergo oxidative addition of methyl iodide to afford **25** (eq 15), and a direct comparison of the two reaction rates under catalytically relevant concentrations showed that oxidative addition outcompetes transmetalation by a substantial factor (Figure 14).

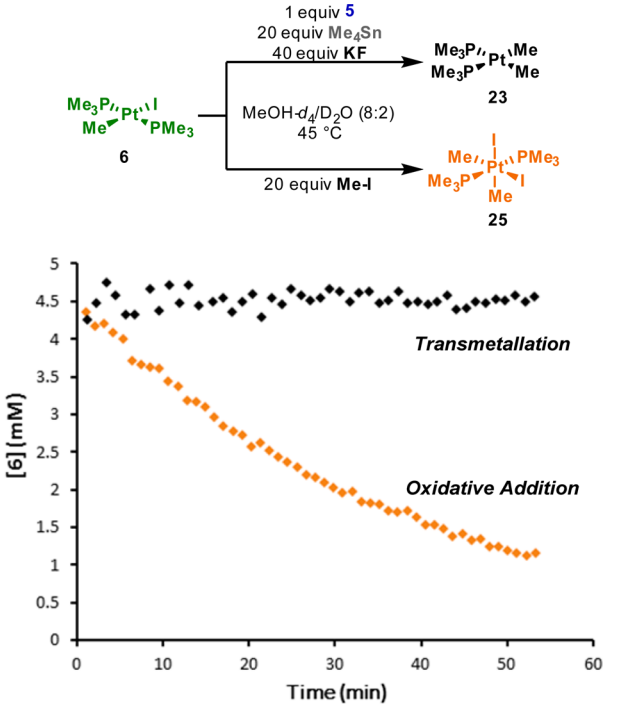

Figure 14. Comparison of the rate for transmetalation with *in situ* generated **24** vs oxidative addition of methyl iodide under catalytically relevant conditions.

This observation led us to more closely examine the behavior of **25**. No reductive elimination was observed in the presence or absence of a supramolecular catalyst. However, in a fashion similar to that observed with **5**, fluoride promoted transmetalation of tetramethyltin to **25** was found to occur to yield **26** and **27**, which could be isolated and fully characterized (eq 16). Complexes **26** and **27** are the *trans*-phosphine analogues of **5** and **24**, but do not undergo detectable thermal isomerization to the thermodynamically favored *cis*-isomers on catalytically relevant time scales.

Moreover, **25** and **27** were observed to conproportionate to yield **26** in the absence of tin, and **26** was observed to disproportionate into **25** and **27** under similar conditions,

DOI: 10.1021/jacs.6b05442
J. Am. Chem. Soc. 2016, 138, 9682−9693

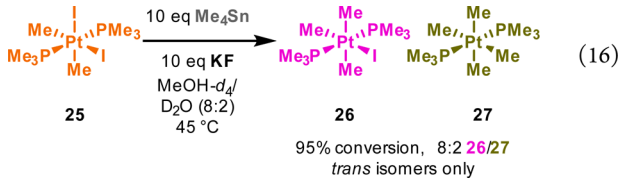

(16)

suggesting that equilibration via Pt(IV)/Pt(IV) methyl transfer is possible under catalytic conditions. This phenomenon was used in the preparation and isolation of **26**.

These observations were surprising given that **26** and **27** are not detectable as intermediates in the dual catalytic reaction. However, treatment of **26** with the supramolecular catalyst **2** leads to rapid consumption of the *trans*- starting material, affording a mixture of *cis*- isomer **5** and reductive elimination product **6**, along with ethane, explaining its low concentration under catalytic conditions (eq 17).

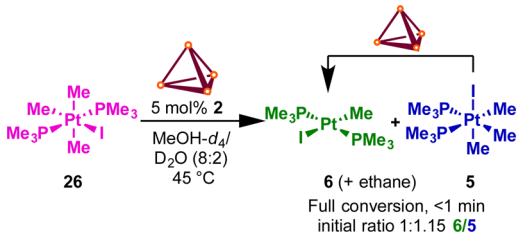

(17)

The reaction was too rapid for accurate monitoring by ^{1}H NMR at the catalytically relevant temperature of 45 °C, but at 25 °C a rate of 2.0×10^{-2} s^{-1} was measured for the combined isomerization/reductive elimination process. For comparison, the pseudo-first-order rate of oxidative addition of methyl iodide to **6** at 45 °C was measured to be 4.38×10^{-4} s^{-1}. This disparity clearly suggests that the failure to detect **26** under catalytic conditions is due to its rapid consumption in the presence of the supramolecular catalyst.

Taken together, these observations suggest an overall mechanism for the process in which the trans-isomers of the Pt(II) and Pt(IV) complexes lie on cycle, with **5** serving as a readily engaged off-cycle resting state and reservoir (Figure 15). Oxidative addition precedes transmetalation, and **26** is rapidly engaged by the supramolecular catalyst.[38] This mechanism is consistent with the observed platinum speciation and suggests that as the concentration of tetramethyltin decreases, the reaction undergoes a shift in the turnover-limiting step (from oxidative addition to transmetalation) and concomitant change in the on-cycle resting state (from **6** to **25**). Additionally consistent is the observation that **6** is a competent precatalyst for this process.[39] Further support is garnered from flooding experiments; when a 10-fold excess of methyl iodide is introduced, **6** is no longer detectable as a persistent intermediate, whereas introduction of a 10-fold excess of tetramethyltin allows **27** to build to detectable levels under catalytic conditions. This mechanism can be used to model the observed concentrations of each platinum species, as well as the tin and alkyl halide species observed under the reaction conditions, using the modeling program COPASI.[40] Table S1 shows the fitted parameters, and Figure S14 shows the agreement of the model with the measured Pt complexes, with the behavior well recapitulated by the proposed mechanism.[39]

IDENTIFICATION OF AN ACIDOLYSIS SIDE REACTION

In addition to the desired cross-product, ethane, small amounts of methane-d_1 were detected by GC-MS of the reaction headspace. Upon examining several potential sources of this side product, it was observed that treatment of **24** with supramolecular complex **1** results in the formation of ethane, methane-d_1, and **23** (eq 18). This reaction is not inhibited by

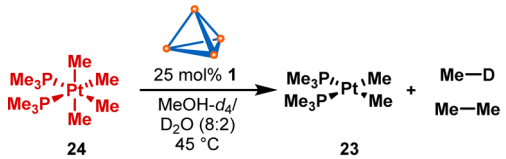

(18)

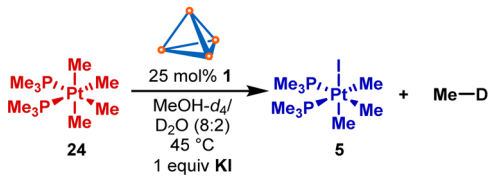

(19)

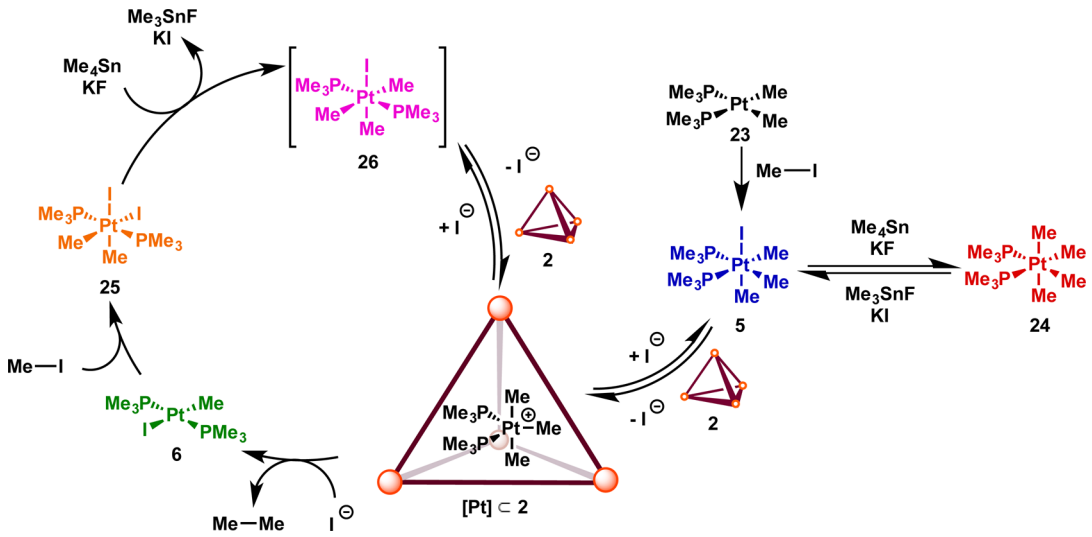

Figure 15. Proposed mechanism for the dual catalytic cross-coupling.[39]

DOI: 10.1021/jacs.6b05442
J. Am. Chem. Soc. 2016, 138, 9682−9693

the addition of fluoride, but the addition of potassium iodide halts the formation of ethane, instead slowly affording a mixture of **5** and methane-d_1 (eq 19). In the absence of catalyst **1**, no significant protonolysis of **24** was observed.

Monitoring the reaction by ^{1}H NMR shows a sigmoidal decay profile for **24**, with formation of **28** as an intermediate en route to **23**. The observed reaction mass balance decreases over the course of the reaction, but can be restored upon the addition of potassium iodide to the completed reaction, affording a mixture of **5** and **6** (Figure 16). These data are

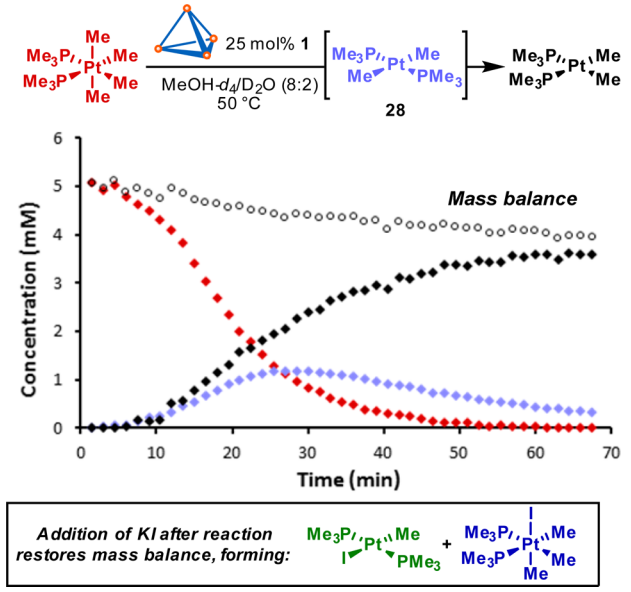

Figure 16. Kinetic profile for the acidolysis of **24** catalyzed by **1**.

consistent with a mechanism involving cluster-promoted acidolysis of **24**,[9] which generates the corresponding cationic trimethyl Pt(IV) complex. Upon cluster-promoted reductive elimination of ethane, the cationic monomethyl Pt(II) complex can abstract a methyl from **24**, continuing the chain reaction (Figure 17). The decrease in mass balance, then, corresponds

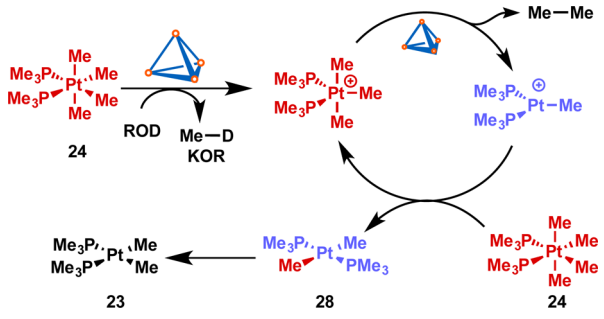

Figure 17. Proposed mechanism for protonolysis-initiated chain reaction.[41]

to the formation of rapidly exchanging unsaturated cationic complexes, either bound within the cluster or free in solution. Similar behavior has previously been observed for Pt(IV) complexes by Puddephatt in the absence of a supramolecular host, wherein initiation occurs by the addition of an extrinsically prepared coordinatively unsaturated cationic Pt(II) complex.[42]

Because the propagation of this pathway is inhibited by iodide, it is unlikely to occur with a significant chain length under catalytic conditions. Furthermore, the substrate for acidolysis (**24**) is present in substantial concentrations only at early reaction times. Nonetheless, this reactivity likely explains some of the observed side-product formation.

CONCLUSIONS

Microenvironment catalysis affords a unique opportunity to transiently modulate the stereoelectronic atmosphere of a catalytic intermediate for one step of a cycle, while leaving the remainder of the cycle unperturbed. In this work, we have thoroughly examined the cationic intermediates preceding, and transition states for carbon−carbon bond-forming, reductive elimination that are recognized by a cocatalytic supramolecular cluster.

The substitutional effects on spectator ligand, halide, reactive group, solvent, and catalyst were systematically explored, and insight into the nature of the resultant Michaelis complex was garnered. A full mechanism for the dual catalytic coupling reaction of alkyl tin and alkyl halide was elucidated on the basis of stoichiometric experiments under catalytically relevant conditions, as well as the mechanism of an acidolysis side reaction.

The strategy outlined herein should be broadly applicable to other elementary steps of interest, and the implementation of other supramolecular catalysts with orthogonal properties and reactivity preferences should allow the extension to other manifolds of reactivity (e.g., transmetalation, oxidative addition, migratory insertion, etc.).[3,4,43] As the instances of this strategy proliferate, catalytic cycles could be developed for which each elementary step is individually engaged by a uniquely tailored microenvironment catalyst. Furthermore, the evolution of more sophisticated supramolecular architectures which are capable of influencing a metal's innate reactivity preferences rather than amplifying them are also surely on the horizon.

ASSOCIATED CONTENT

Supporting Information

The Supporting Information is available free of charge on the ACS Publications website at DOI: 10.1021/jacs.6b05442.

Experimental details, characterization data, and COPASI model (PDF)
X-ray data (**9** ⊂ **1**) (CIF)
X-ray data (**25**) (CIF)

AUTHOR INFORMATION

Corresponding Authors

*rbergman@berkeley.edu
*raymond@socrates.berkeley.edu
*fdtoste@berkeley.edu

Author Contributions

†M.D.L. and D.M.K. contributed equally.

Notes

The authors declare no competing financial interest.

ACKNOWLEDGMENTS

This research was supported by the Director, Office of Science, Office of Basic Energy Sciences and the Division of Chemical Sciences, Geosciences, and Biosciences of the U.S. Department of Energy at Lawrence Berkeley National Laboratory (Grant

DOI: 10.1021/jacs.6b05442
J. Am. Chem. Soc. 2016, 138, 9682−9693

DE-AC02-05CH11231) and NIH National Institute of General Medical Sciences (Grant R01 GM073932) for funding. M.D.L. thanks the NSF GRFP program and ARCS foundation for graduate fellowships. D.M.K. was supported by an NSF GRFP (Grant No. DGE 1106400). The Advanced Light Source is supported by the Director, Office of Science, Office of Basic Energy Sciences, of the U.S. Department of Energy under Contract No. DE-AC02-05CH11231. We thank Dr. Derek Dalton, Dr. William Wolf, Dr. Matthew Winston, and Suhong Kim for helpful discussions and Dr. William Wolf and Dr. Simon Clark for assistance with crystallographic analyses. The Tilley and Arnold groups are thanked for experimental assistance with carbon monoxide.

REFERENCES

(1) Hartwig, J. F. *Organotransition Metal Chemistry: From Bonding to Catalysis*; University Science Books: 2010.

(2) For reviews on ligand effects on transition metal catalysis: (a) Tolman, C. A. *Chem. Rev.* **1977**, *77* (3), 313. (b) Berrisford, D. J.; Bolm, C.; Sharpless, K. B. *Angew. Chem., Int. Ed. Engl.* **1995**, *34* (10), 1059. (c) van Leeuwen, P. W. N. M.; Kamer, P. C. J.; Reek, J. N. H.; Dierkes, P. *Chem. Rev.* **2000**, *100* (8), 2741. (d) Surry, D. S.; Buchwald, S. L. *Angew. Chem., Int. Ed.* **2008**, *47* (34), 6338. (e) Hartwig, J. F. *Acc. Chem. Res.* **2008**, *41* (11), 1534. (f) Fu, G. C. *Acc. Chem. Res.* **2008**, *41* (11), 1555.

(3) For reviews on supramolecular microenvironment catalysis: (a) Cram, D. J.; Cram, J. M. *Science* **1974**, *183* (4127), 803. (b) Meeuwissen, J.; Reek, J. N. H. *Nat. Chem.* **2010**, *2* (8), 615. (c) Brown, C. J.; Toste, F. D.; Bergman, R. G.; Raymond, K. N. *Chem. Rev.* **2015**, *115* (9), 3012. (d) Yoshizawa, M.; Klosterman, J. K.; Fujita, M. *Angew. Chem., Int. Ed.* **2009**, *48* (19), 3418. (e) Catti, L.; Zhang, Q.; Tiefenbacher, K. *Synthesis* **2016**, *48*, 313. For reviews related to noncovalent interaction in catalysis: (f) Zhao, Y.; Cotelle, Y.; Sakai, N.; Matile, S. *J. Am. Chem. Soc.* **2016**, *138*, 4270. (g) Knowles, R. R.; Jacobsen, E. J. *Proc. Natl. Acad. Sci. U. S. A.* **2010**, *107*, 20678. (h) Wheeler, S. E.; Seguin, T. J.; Guan, Y.; Doney, A. C. *Acc. Chem. Res.* **2016**, *49*, 1061. (i) Wiester, M. J.; Ulmann, P. A.; Mirkin, C. A. *Angew. Chem., Int. Ed.* **2011**, *50*, 114. (j) Raynal, M.; Ballester, P.; Vidal-Ferran, A.; van Leeuwen, P. W. N. M. *Chem. Soc. Rev.* **2014**, *43*, 1734. (k) Leenders, S. H. A. M.; Gramage-Doria, R.; de Bruin, B.; Reek, J. N. H. *Chem. Soc. Rev.* **2015**, *44*, 433. (l) Koblenz, T. S.; Wassenaar, J.; Reek, J. N. H. *Chem. Soc. Rev.* **2008**, *37*, 247. For reviews pertaining to dual catalysis and cooperative interactions: (m) Allen, A. E.; MacMillan, D. W. C *Chem. Sci.* **2012**, *3*, 633. (n) Ambrosini, L. M.; Lambert, T. H. *ChemCatChem* **2010**, *2*, 1373. (o) Hopkinson, M. N.; Sahoo, B.; Li, J.; Glorius, F. *Chem. - Eur. J.* **2014**, *20*, 3874.

(4) Selected examples of supramolecular microenvironment catalysis: (a) Salles, A. G.; Zarra, S.; Turner, R. M.; Nitschke, J. R. *J. Am. Chem. Soc.* **2013**, *135* (51), 19143. (b) Yoshizawa, M.; Tamura, M.; Fujita, M. *Science* **2006**, *312* (5771), 251. (c) Cullen, W.; Misuraca, M. C.; Hunter, C. A.; Williams, N. H.; Ward, M. D. *Nat. Chem.* **2016**, *8* (3), 231. (d) Zhang, Q.; Tiefenbacher, K. *Nat. Chem.* **2015**, *7* (3), 197.

(5) Kaphan, D. M.; Levin, M. D.; Bergman, R. G.; Raymond, K. N.; Toste, F. D. *Science* **2015**, *350* (6265), 1235.

(6) Caulder, D. L.; Powers, R. E.; Parac, T. N.; Raymond, K. N. *Angew. Chem., Int. Ed.* **1998**, *37* (13−14), 1840.

(7) Zhao, C.; Sun, Q.-F.; Hart-Cooper, W. M.; DiPasquale, A. G.; Toste, F. D.; Bergman, R. G.; Raymond, K. N. *J. Am. Chem. Soc.* **2013**, *135* (50), 18802.

(8) (a) Davis, A. V.; Raymond, K. N. *J. Am. Chem. Soc.* **2005**, *127* (21), 7912. (b) Biros, S. M.; Bergman, R. G.; Raymond, K. N. *J. Am. Chem. Soc.* **2007**, *129* (40), 12094. (c) Parac, T. N.; Caulder, D. L.; Raymond, K. N. *J. Am. Chem. Soc.* **1998**, *120* (31), 8003. (d) Leung, D. H.; Bergman, R. G.; Raymond, K. N. *J. Am. Chem. Soc.* **2008**, *130* (9), 2798.

(9) Pluth, M. D.; Bergman, R. G.; Raymond, K. N. *J. Am. Chem. Soc.* **2007**, *129* (37), 11459.

(10) (a) Kaphan, D. M.; Toste, F. D.; Bergman, R. G.; Raymond, K. N. *J. Am. Chem. Soc.* **2015**, *137* (29), 9202. (b) Hart-Cooper, W. M.; Clary, K. N.; Toste, F. D.; Bergman, R. G.; Raymond, K. N. *J. Am. Chem. Soc.* **2012**, *134* (43), 17873. (c) Pluth, M. D.; Bergman, R. G.; Raymond, K. N. *Science* **2007**, *316* (5821), 85. (d) Fiedler, D.; Bergman, R. G.; Raymond, K. N. *Angew. Chem., Int. Ed.* **2004**, *43* (48), 6748. (e) Zhao, C.; Toste, F. D.; Raymond, K. N.; Bergman, R. G. *J. Am. Chem. Soc.* **2014**, *136* (41), 14409.

(11) (a) Wang, Z. J.; Brown, C. J.; Bergman, R. G.; Raymond, K. N.; Toste, F. D. *J. Am. Chem. Soc.* **2011**, *133* (19), 7358. (b) Wang, Z. J.; Clary, K. N.; Bergman, R. G.; Raymond, K. N.; Toste, F. D. *Nat. Chem.* **2013**, *5* (2), 100. (c) Fiedler, D.; Bergman, R. G.; Raymond, K. N. *Angew. Chem., Int. Ed.* **2006**, *45* (5), 745. (d) Fiedler, D.; Pagliero, D.; Brumaghim, J. L.; Bergman, R. G.; Raymond, K. N. *Inorg. Chem.* **2004**, *43* (3), 846. (e) Leung, D. H.; Fiedler, D.; Bergman, R. G.; Raymond, K. N. *Angew. Chem., Int. Ed.* **2004**, *43* (8), 963. (f) Leung, D. H.; Bergman, R. G.; Raymond, K. N. *J. Am. Chem. Soc.* **2007**, *129* (10), 2746. (g) Fiedler, D.; Leung, D. H.; Bergman, R. G.; Raymond, K. N. *Acc. Chem. Res.* **2005**, *38* (4), 349. (h) Leung, D. H.; Bergman, R. G.; Raymond, K. N. *J. Am. Chem. Soc.* **2006**, *128* (30), 9781. (i) Fiedler, D.; Leung, D. H.; Bergman, R. G.; Raymond, K. N. *J. Am. Chem. Soc.* **2004**, *126* (12), 3674.

(12) (a) Komiya, S.; Kochi, J. K. *J. Am. Chem. Soc.* **1976**, *98* (24), 7599. (b) Komiya, S.; Albright, T. A.; Hoffmann, R.; Kochi, J. K. *J. Am. Chem. Soc.* **1976**, *98* (23), 7255. (c) Tamaki, A.; Kochi, J. K. *J. Organomet. Chem.* **1974**, *64* (3), 411. (d) Tamaki, A.; Kochi, J. K. *J. Organomet. Chem.* **1972**, *40* (2), C81.

(13) (a) Brown, M. P.; Puddephatt, R. J.; Upton, C. E. E. *J. Chem. Soc., Dalton Trans.* **1974**, *22*, 2457. (b) Goldberg, K. I.; Yan, J. Y.; Winter, E. L. *J. Am. Chem. Soc.* **1994**, *116* (4), 1573. (c) Goldberg, K. I.; Yan, J.; Breitung, E. M. *J. Am. Chem. Soc.* **1995**, *117* (26), 6889.

(14) Pseudo-zero-order initial rates are used for reductive elimination from **3-I** and **5** because of deviation from first-order kinetics as a result of catalyst deactivation (vide infra).

(15) Lineweaver, H.; Burk, D. *J. Am. Chem. Soc.* **1934**, *56* (3), 658.

(16) In the case of triethylphosphine congener **7-I**, no catalyst deactivation is observed, allowing the comparison of the catalyzed and uncatalyzed rates using a first-order kinetic model. Indeed, the rapid consumption of **7-I** in the catalyzed reaction renders analysis by initial rates impractical. For this reason, in order to compare the pseudo-zero-order initial rate constants for **3-I** and **5** to the first-order rate constant for **7-I**, one must multiply the first-order rate constant by the initial concentration of **7-I**.

(17) While investigation of the contribution of the specific noncovalent interactions to transition state recognition and stabilization within cluster **1** is beyond the purview of this report, a previous study of **1** in the context of related catalytic systems, as well as the thermodynamics of guest complexation, suggests contribution from many sources including entropic gains from cation and host desolvation, Coulombic stabilization, and cation−π interactions. See ref 8d, 11h, and: (a) Sgarlata, C.; Mugridge, J. S.; Pluth, M. D.; Tiedemann, B. E. F.; Zito, V.; Arena, G.; Raymond, K. *J. Am. Chem. Soc.* **2010**, *132*, 1005. (b) Hastings, C. J.; Bergman, R. G.; Raymond, K. N. *Chem. - Eur. J.* **2014**, *20*, 3966.

(18) Mecozzi, S.; Rebek, J., Jr. *Chem. - Eur. J.* **1998**, *4* (6), 1016.

(19) Schuster, O.; Schmidbaur, H. *Z. Naturforsch., B: J. Chem. Sci.* **2006**, *61* (1), 1.

(20) For size exclusion in supramolecular catalysis: (a) Pluth, M. D.; Bergman, R. G.; Raymond, K. N. *J. Am. Chem. Soc.* **2008**, *130* (34), 11423. (b) Lee, S. J.; Cho, S.-H.; Mulfort, K. L.; Tiede, D. M.; Hupp, J. T.; Nguyen, S. T. *J. Am. Chem. Soc.* **2008**, *130* (50), 16828. (c) Ryu, E.-H.; Cho, H.; Zhao, Y. *Org. Lett.* **2007**, *9* (25), 5147.

(21) For size exclusion in enzymes: (a) Koshland, D. E. *Proc. Natl. Acad. Sci. U. S. A.* **1958**, *44* (2), 98. (b) Johnson, K. A. *J. Biol. Chem.* **2008**, *283* (39), 26297.

(22) To calculate the heterolytic bond strengths, the differences in homolytic bond strengths were combined with the differences in

DOI: 10.1021/jacs.6b05442
J. Am. Chem. Soc. 2016, 138, 9682−9693

electron affinity for the halides, treating the dissociated neutral atoms as isoenergetic. The ionization potential of gold can be omitted from the calculation because the energies are relative. The results are that, in a heterolytic sense, the Au—Cl bond is approximately 9 kcal/mol stronger than the Au—Br bond which is approximately 11 kcal/mol more stable than the Au—I bond. For the Au(III) BDE: (a) Winston, M. S.; Wolf, W. J.; Toste, F. D. *J. Am. Chem. Soc.* **2015**, *137* (24), 7921. For the electron affinities of Cl, Br, and I: (b) Berzinsh, U.; Gustafsson, M.; Hanstorp, D.; Klinkmueller, A.; Ljungblad, U.; Martensson-Pendrill, A.-M. *Phys. Rev. A: At., Mol., Opt. Phys.* **1995**, *51* (1), 231−238. (c) Blondel, C.; Cacciani, P.; Delsart, C.; Trainham, R. *Phys. Rev. A: At., Mol., Opt. Phys.* **1989**, *40* (7), 3698−3701. (d) Pelaez, R. J.; Blondel, C.; Delsart, C.; Drag, C. *J. Phys. B: At., Mol. Opt. Phys.* **2009**, *42*, 125001−125007.

(23) (a) Slansky, C. M. *J. Am. Chem. Soc.* **1940**, *62* (9), 2430. (b) Morris, D. F. C. *Struct. Bonding (Berlin)*; Springer Berlin Heidelberg: Berlin, Heidelberg, 1968; pp 63−82.

(24) Again the homolytic bond dissociation energies were combined with the electron affinity of the halides (ref 19b−d) to arrive at the heterolytic BDE values. Though the error bars given for the BDE values (± 7 kcal for Au—I) limit the certainty of such an analysis, the results are that, in a heterolytic sense, the Au—I bond is approximately 6 kcal/mol stronger than the Au—Cl bond which is approximately 10 kcal/mol more stable than the Au—Br bond. For the homolytic dissociation energies, see: Brown, J. R.; Schwerdtfeger, P.; Schröder, D.; Schwarz, H. *J. Am. Soc. Mass Spectrom.* **2002**, *13* (5), 485.

(25) For d^8 metal reductive elimination: (a) Wolf, W. J.; Winston, M. S.; Toste, F. D. *Nat. Chem.* **2013**, *6* (2), 159. (b) Tatsumi, K.; Hoffmann, R.; Yamamoto, A.; Stille, J. K. *Bull. Chem. Soc. Jpn.* **1981**, *54*, 1857. (c) Gillie, A.; Stille, J. K. *J. Am. Chem. Soc.* **1980**, *102* (15), 4933. (d) Levin, M. D.; Toste, F. D. *Angew. Chem., Int. Ed.* **2014**, *53* (24), 6211. (e) Joost, M.; Amgoune, A.; Bourissou, D. *Angew. Chem., Int. Ed.* **2015**, *54* (50), 15022.

(26) For d^6 metal reductive elimination: (a) Roy, S.; Puddephatt, R. J.; Scott, J. D. *J. Chem. Soc., Dalton Trans.* **1989**, *11*, 2121. (b) Crumpton-Bregel, D. M.; Goldberg, K. I. *J. Am. Chem. Soc.* **2003**, *125* (31), 9442. (c) Deutsch, P. P.; Eisenberg, R. *J. Am. Chem. Soc.* **1990**, *112* (2), 714. (d) Buchanan, J. M.; Stryker, J. M.; Bergman, R. G. *J. Am. Chem. Soc.* **1986**, *108* (7), 1537. (e) Harper, T. G. P.; Desrosiers, P. J.; Flood, T. C. *Organometallics* **1990**, *9* (9), 2523.

(27) We have employed varying ratios of potential guests and cluster due to differing distributions of encapsulated species. The selected stoichiometries displayed reflect those which afforded the clearest illustration of the encapsulation behavior.

(28) (a) Forniés, J.; Gómez-Saso, M. A.; Martín, A.; Martínez, F.; Menjón, B.; Navarrete, J. *Organometallics* **1997**, *16* (26), 6024. (b) Scott, J. D.; Puddephatt, R. J. *Organometallics* **1986**, *5* (6), 1253. (c) Howard, W. A.; Bergman, R. G. *Polyhedron* **1998**, *17*, 803. (d) Martínez-Salvador, S.; Forniés, J.; Martín, A.; Menjón, B. *Chem. - Eur. J.* **2011**, *17* (29), 8085.

(29) This complex was isolated as a mixture of isomers. See the SI for details.

(30) Brown, M. P.; Puddephatt, R. J.; Upton, C. E. E.; Lavington, S. W. *J. Chem. Soc., Dalton Trans.* **1974**, *15*, 1613.

(31) We cannot distinguish conclusively between this isomer and the alternative achiral complex bearing *trans* phosphines based on ^{1}H NMR, but have based our tentative assignment on the chemical shifts of complexes **24**, **26**, and **27**, in which mutually *trans* methyl groups show a substantial upfield shift compared to methyl groups trans to phosphine or halide groups.

(32) Hart-Cooper, W. M.; Zhao, C.; Triano, R. M.; Yaghoubi, P.; Ozores, H. L.; Burford, K. N.; Toste, F. D.; Bergman, R. G.; Raymond, K. N. *Chem. Sci.* **2015**, *6* (2), 1383.

(33) Examples of alkyl stannane transmetalation to Pt: (a) Romeo, R.; Scolaro, L. M.; Catalano, V.; Achar, S. *Inorganic Syntheses*; John Wiley & Sons, Inc.: 2007; pp 153−158. (b) Clark, H. C.; Goel, A. B.; Jain, V. K.; Tyers, K. G.; Wong, C. S. *J. Organomet. Chem.* **1987**, *321* (1), 123. (c) Rakowsky, M. H.; Woolcock, J. C.; Rettig, M. F.; Wing, R. M. *Organometallics* **1988**, *7* (10), 2149. (d) Dekker, G. P. C. M.; Buijs, A.; Elsevier, C. J.; Vrieze, K.; Van Leeuwen, P. W. N. M.; Smeets, W. J. J.; Spek, A. L.; Wang, Y. F.; Stam, C. H. *Organometallics* **1992**, *11* (5), 1937. (e) Nilsson, P.; Plamper, F.; Wendt, O. F. *Organometallics* **2003**, *22* (25), 5235.

(34) In the absence of the supramolecular catalyst, only **5** and **24** are observed.

(35) (a) Hux, J. E.; Puddephatt, R. J. *Inorg. Chim. Acta* **1985**, *100* (1), 1. (b) Lashanizadehgan, M.; Rashidi, M.; Hux, J. E.; Puddephatt, R. J.; Ling, S. S. M. *J. Organomet. Chem.* **1984**, *269* (3), 317.

(36) Treatment of **24** with methanolic trimethyltin fluoride in the absence of potassium iodide results in the formation of two different trimethyl-Pt(IV) species which are not sufficiently stable for isolation. We speculate that these are the Pt(IV) fluoride and solvato complexes, but cannot definitively assign them at this time.

(37) (a) Herzog, A.; Liu, F.-Q.; Roesky, H. W.; Demsar, A.; Keller, K.; Noltemeyer, M.; Pauer, F. *Organometallics* **1994**, *13* (4), 1251. (b) Vela, J.; Smith, J. M.; Yu, Y.; Ketterer, N. A.; Flaschenriem, C. J.; Lachicotte, R. J.; Holland, P. L. *J. Am. Chem. Soc.* **2005**, *127* (21), 7857. (c) Ding, K.; Dugan, T. R.; Brennessel, W. W.; Bill, E.; Holland, P. L. *Organometallics* **2009**, *28* (23), 6650.

(38) We cannot definitively exclude the possibility that transmetalation from **24** to **6** is followed by rapid oxidative addition, but the observed build-up of **25** and fast decrease in concentration of **24** suggest that such a pathway is only potentially catalytically relevant at early reaction times. Similarly, we cannot definitively exclude the possibility that the kinetic product of reductive elimination is the *cis* isomer of **6**, and that a competition between isomerization to **6** and either oxidative addition (to give a *cis* isomer of **25**) or transmetalation (to give **23**) establishes a parallel catalytic cycle involving only *cis*-phosphine isomers. Here, the kinetic invisibility of the *cis* isomer of **6** in the cluster catalyzed stoichiometric reductive elimination suggests that such a pathway is unlikely to dominate over the proposed mechanism.

(39) See SI for Details.

(40) Hoops, S.; Sahle, S.; Gauges, R.; Lee, C.; Pahle, J.; Simus, N.; Singhal, M.; Xu, L.; Mendes, P.; Kummer, U. *Bioinformatics* **2006**, *22* (24), 3067.

(41) The stereochemistry of the encapsulated coordinatively unsaturated platinum cation is unknown and may be any of a number of trigonal bipyramidal or square pyramidal isomers, though as with other five coordinate transition metal complexes it is expected to be rapidly stereochemically fluxional.

(42) (a) Hill, G. S.; Puddephatt, R. J. *Organometallics* **1997**, *16* (21), 4522. (b) Hill, G. S.; Yap, G. P. A.; Puddephatt, R. J. *Organometallics* **1999**, *18* (8), 1408.

(43) A variety of catalytically active supramolecular assemblies besides **1** and **2** have been reported: (a) Szabo, T.; Hilmersson, G.; Rebek, J. *J. Am. Chem. Soc.* **1998**, *120* (24), 6193. (b) Takeda, N.; Umemoto, K.; Yamaguchi, K.; Fujita, M. *Nature* **1999**, *398* (6730), 794. (c) Mal, P.; Schultz, D.; Beyeh, K.; Rissanen, K.; Nitschke, J. R. *Angew. Chem., Int. Ed.* **2008**, *47* (43), 8297. (d) Liu, S.; Gibb, B. C. *Chem. Commun.* **2008**, *32*, 3709. (e) Tidmarsh, I. S.; Faust, T. B.; Adams, H.; Harding, L. P.; Russo, L.; Clegg, W.; Ward, M. D. *J. Am. Chem. Soc.* **2008**, *130* (45), 15167. (f) Merlau, M. L.; del Pilar Mejia, M.; Nguyen, S. T.; Hupp, J. T. *Angew. Chem., Int. Ed.* **2001**, *40* (22), 4239.

DOI: 10.1021/jacs.6b05442
J. Am. Chem. Soc. 2016, 138, 9682−9693